Electric Field inside a Hole-Only Device and Insights into Space-Charge-Limited Current Measurement for Organic Semiconductors

ARTICLE *in* THE JOURNAL OF PHYSICAL CHEMISTRY C · APRIL 2014

Impact Factor: 4.77 · DOI: 10.1021/jp5035618

4 AUTHORS, INCLUDING:

Haoyuan Li
Tsinghua University
17 PUBLICATIONS **114** CITATIONS

SEE PROFILE

THE JOURNAL OF PHYSICAL CHEMISTRY C

Article

pubs.acs.org/JPCC

Electric Field inside a Hole-Only Device and Insights into Space-Charge-Limited Current Measurement for Organic Semiconductors

Haoyuan Li, Lian Duan,* Deqiang Zhang, and Yong Qiu

Key Lab of Organic Optoelectronics and Molecular Engineering of Ministry of Education, Department of Chemistry, Tsinghua University, Beijing, 100084, China

Supporting Information

ABSTRACT: It is known that the electric field is nonuniform inside organic electronic devices. However, the physics a few nanometers near interfaces and factors that influence the electric field distribution are still not fully understood. Moreover, the mobility might be nonuniform inside the device, since it is electric-field dependent. However, this has been overlooked in the apprehension of the space-charge-limited (SCL) current in the commonly used Mott−Gurney equation. Here, we carry out 3D multiparticle Monte Carlo simulations to study the electric field and energy diagram in a hole-only device under bias. Coulomb potential is obtained from the solution of the 1D Poisson equation of our system. The influences of the injection barrier, the energetic disorder and the applied bias are studied in detail. The SCL current is compared with that from the Mott−Gurney equation. It is found that the apparent charge mobilities are close to those calculated using the transit time corresponding to the cross point of asymptotes to the plateau and trailing edge of the current in the double logarithmic plot in the time-of-flight (TOF) simulations, which means that the space-charge-limited current (SCLC) measurement can be reliable for organic semiconductors.

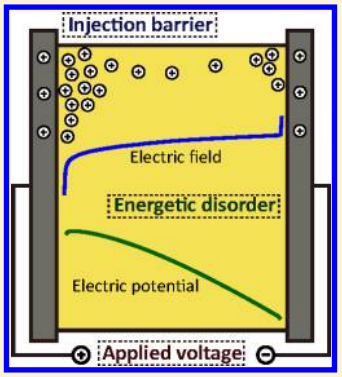

INTRODUCTION

Organic electronic devices are widely used in research and industry.[1−4] However, the physics in them, which is of crucial importance to the design of better ones is still not fully understood. Devices such as organic light-emitting diodes (OLEDs) are driven by an applied voltage. Electrons and holes moving under the electric field is the most fundamental physical process. The involvement of charge carriers will lead to perturbation in the electric potential, which means that the electric field is nonuniform. This inhomogeneity is considered to have a significant influence on the performance of devices.[5,6]

Organic electronic devices typically have a thickness of several hundred nanometers, making obtaining the complete information on their interior difficult from experiment. Electroabsorption (EA) technique has been widely applied and shows that the electric field varies in different layers of diodes.[7−9] The use of a metal bridge can also reveal electric potential inside a device.[10,11] However, the electric field distribution a few nanometers near interfaces, which has a great influence on the charge transport process, is difficult to probe. Using numerical methods, Tutiš and van Mensfoort et al. have shown weakened electric field near the injecting electrode.[12,13] However, the energy diagram inside the device and factors that affect the electric field distribution are still not fully understood.

The space-charge-limited (SCL) current in organic semiconductors is often apprehended using the Mott−Gurney equation, which assumes a constant mobility and negligible diffusion. In our previous work it has been shown that these assumptions are inappropriate for the charge transport in organic semiconductors.[14,15] Moreover, because of the nonuniform electric field in the device, the mobility is also inhomogeneous, which is not considered in the Mott−Gurney equation. Nevertheless, it is widely used in the space-charge-limited current (SCLC) experiment to calculate charge mobilities of organic semiconductors.[16−22] In 2008, using 1D drift-diffusion simulations with electric-field and carrier-density dependent charge mobility, van Mensfoort and co-workers found that the Mott−Gurney equation underestimates the current density.[13] However, the meaning of the extracted charge mobilities from the SCL currents and whether we should compare them with those from other measurements remains unclear.

Here, we investigate the influence of the energetic disorder of the system, the injection barrier and the applied voltage on the internal electric field to help establish a better description of the physics in organic electronic devices. In order to achieve this, we emulate a hole-only device using 3D multiparticle Monte Carlo simulations, which proves reliable to study the charge transport in organic semiconductors.[23−32] The current density of the device is calculated and compared with that described by the commonly used Mott−Gurney equation. The exacted mobilities are compared with those from the time-of-flight (TOF) simulations, which we hope will help researchers better understand the SCLC measurement of organic semiconductors.

Received: April 11, 2014
Published: April 17, 2014

dx.doi.org/10.1021/jp5035618 | J. Phys. Chem. C 2014, 118, 9990−9995

THEORETICAL BASIS AND COMPUTATIONAL DETAILS

Our simulated device is represented by a 3D grid of 70 × 70 × 210 sites, where the site energy conforms to Gaussian distribution. The site distance a is set to 1.6 nm, a value found by Pasveer and co-workers.[33] Periodic boundary condition is applied in x and y directions, and the electric field is applied in the z direction. The simulated system represents a 334 nm hole-only device.

Charge transport in organic semiconductors can be described by successive hops between molecules.[34−36] In our simulations, carriers hop one at a time. Every step, the one which causes the shortest advancement of the global time moves.[37−39] In the case of weak electron−phonon coupling, the Miller−Abrahams equation can be used to calculate the phonon-assisted hopping rate:[40]

$$\nu_{ij} = \nu_0 \exp(-2\gamma|R_{ij}|)\begin{cases}\exp\left(-\dfrac{\varepsilon_j - \varepsilon_i}{k_B T}\right) & \varepsilon_j > \varepsilon_i \\ 1 & \varepsilon_j \le \varepsilon_i\end{cases} \quad (1)$$

where ν_0 is the phonon vibration frequency, γ is the inverse localization radius and is set to $5/a$,[34] R_{ij} is the distance from site i to j, k_B is the Boltzmann constant, T is the temperature, and ε_i and ε_j are the energy levels of the respective sites.

In amorphous organic materials, the molecules are often largely localized, and charges can be considered to be only able to transfer to the nearest neighbors. In the simulations, we choose a cubic area consisting of 3 × 3 × 3 sites, centering on the site that has the carrier, that is, a maximum hopping distance of $\sqrt{3}a$ is allowed. The carrier dwell time on one molecule t_i and the hopping direction k are calculated as follows:[41,42]

$$t_i = -\frac{\ln(\xi_1)}{\sum_j \nu_{ij}} \quad (2)$$

$$\frac{\sum_{j=1}^{k-1}\nu_{ij}}{\sum_j \nu_{ij}} < \xi_2 \le \frac{\sum_{j=1}^{k}\nu_{ij}}{\sum_j \nu_{ij}} \quad (3)$$

where ξ_1 and ξ_2 are random numbers uniformly distributed between 0 and 1.

Layers z = 1 and z = 210 are set as the anode and the cathode, respectively. Before simulation, a fixed number of sites on them are chosen as injection spots. The injection rate is calculated using eq 1.[39] Whenever a carrier moves from an injection spot to the interior, a new carrier is spawned at this very spot. Other than this, injection is treated the same way as hops elsewhere. Hopping back into electrodes is allowed. Carriers are removed outside the system upon reaching the anode or the cathode. The hole-only device is considered to be symmetric. This means that the number of injection spots and the injection barrier (if it exists) are the same at both electrodes.

Resistance in the outer circuit is omitted, which means $\Delta\varphi \equiv V$, where $\Delta\varphi$ is the potential difference between the two electrodes and V is the applied voltage. Coulomb potential is treated by solving the 1D Poisson equation in the z direction. Here, we give the solution of our system as

$$\phi_i = -\sum_l^N \frac{\rho_l d_{i,l}}{2\varepsilon_0\varepsilon_r} + \sum_l^N \frac{\rho_l d_{1,l}}{2\varepsilon_0\varepsilon_r} - \left[V - \left(-\sum_l^N \frac{\rho_l d_{1,l}}{2\varepsilon_0\varepsilon_r} + \sum_l^N \frac{\rho_l d_{N,l}}{2\varepsilon_0\varepsilon_r}\right)\right]\frac{d_{i,1}}{d_{N,1}} \quad (4)$$

where ρ_l is the charge density at layer $z = l$, $d_{i,l}$ is the distances between i to l, N is 210 for our system, ε_0 is the vacuum permittivity, and ε_r is the relative permittivity which is set to 4, a value commonly found in organic materials.[41] Practically, the electric potential difference between two sites are calculated the same way as in our previous work,[14,15] which is identical to the use of eq 4.

After a hop, carrier dwell times of all affected carriers are recalculated. The number of carriers, and the electric potential at different positions in the z direction are recorded at a fixed time interval. Results are obtained by averaging over enough time.

RESULTS AND DISCUSSION

Figure 1a−f show the distribution of carriers near the anode at different injection barriers Δ and energetic disorders σ. It can

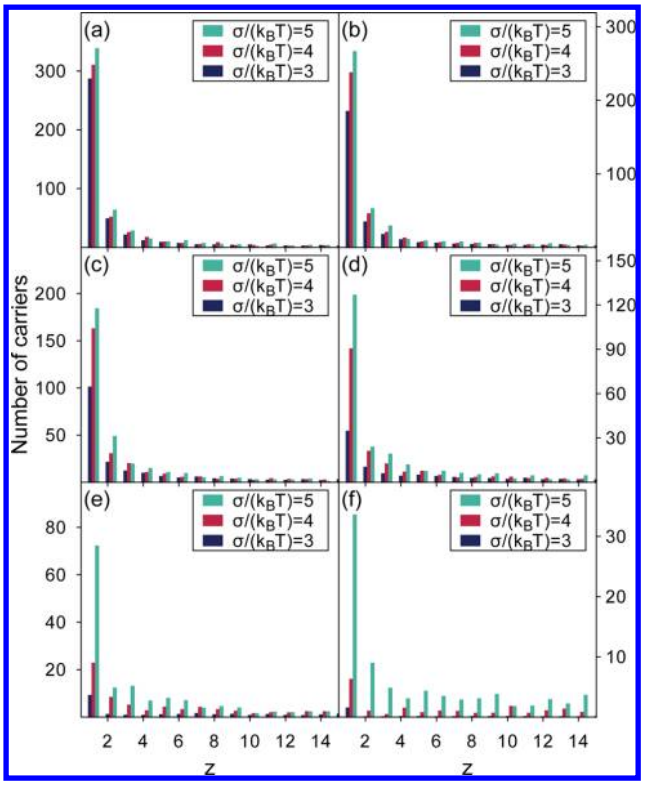

Figure 1. Number of carriers near the anode for an injection barrier of (a) 0, (b) 0.1, (c) 0.2, (d) 0.3, (e) 0.4, and (f) 0.5 eV. The applied electric field is 3 × 10^5 V/cm.

be seen that at smaller Δ, more carriers are injected and accumulated near the anode. These carriers seem difficult to drift toward the cathode. They act as a reservoir, as if carriers are drawn from it instead of directly from the anode. This is in consistency with the results from numerical simulations.[12,13] Increasing the energetic disorder enlarges this reservoir. This can be understood that when σ is higher, injection is enhanced since more sites have lower energy where charges at the

dx.doi.org/10.1021/jp5035618 | J. Phys. Chem. C 2014, 118, 9990−9995

electrode can hop to. Furthermore, carriers drift slower at higher $\sigma/(k_BT)$, leading to more accumulated carriers.

The electric field across the device is shown in Figure 2a–f. We can see that it is highly nonuniform. The electric field is

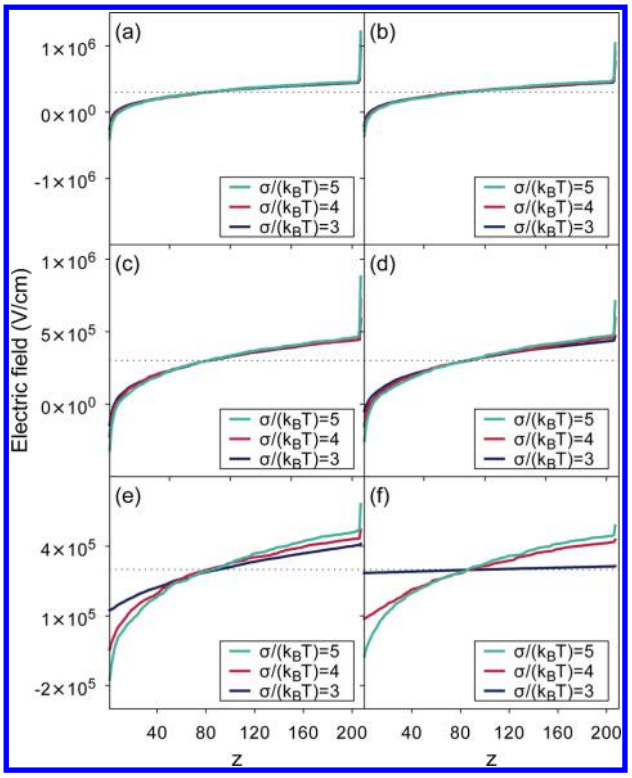

Figure 2. Electric field across the device for an injection barrier of (a) 0, (b) 0.1, (c) 0.2, (d) 0.3, (e) 0.4, and (f) 0.5 eV. Dotted lines indicate the applied electric field (3×10^5 V/cm).

much lower near the anode, due to the influence of the space-charge perturbation. This phenomenon has also been shown by Tutiš and van Mensfoort et al.[12,13] At small Δ, an inversion area appears near the anode, where the electric field changes polarity. This suppresses further injection and slows carrier motion toward the cathode. In fact, because the electric field is reversed at this part, most carriers drift toward the anode, and only a small portion can diffusive away. At the other side of the device, however, the electric field slowly increases and exceeds the applied one. This means that the carrier motion is slow near the anode, while carriers gradually speed up when they move away. Upon increasing the injection barrier, this degree of inhomogeneity decreases. For $\sigma/(k_BT) = 3$, when $\Delta = 0.5$ eV, the electric field becomes uniform again. However, the injection barrier has a smaller effect for systems with higher energetic disorders. For $\sigma/(k_BT) = 5$, the electric field is still highly nonuniform even at $\Delta = 0.5$ eV. The reason is that in these cases, carriers are easier to accumulate near the electrode, as shown in Figure 1a–f.

Figure 3a–f shows the electric potential across the sample. It can be seen that a barrier forms near the anode for low-to-medium injection degrees, which is caused by the space charge of the accumulated carriers. The barrier height increases with the degree of inhomogeneity of the electric field. For a small energetic disorder, the potential surface becomes linear again at large Δ, as shown in Figure 3f. The concave curve is in

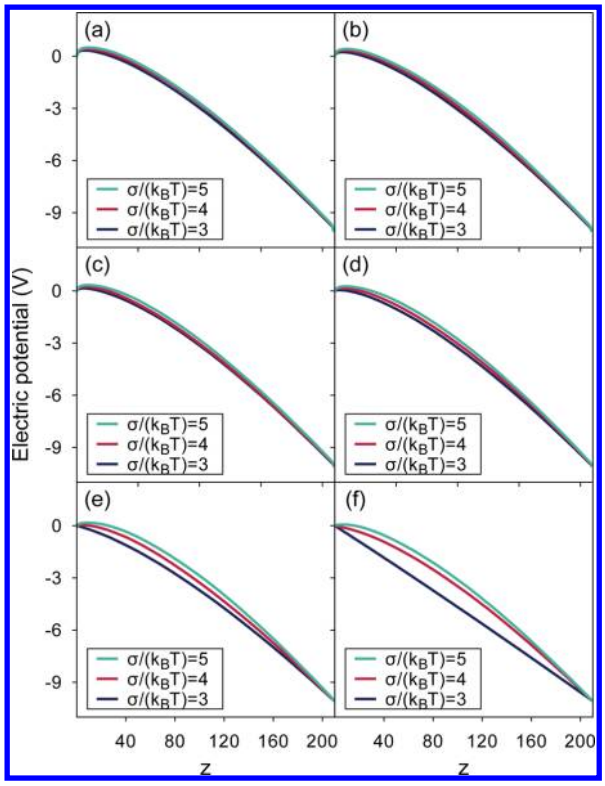

Figure 3. Electric potential across the device for an injection barrier of (a) 0, (b) 0.1, (c) 0.2, (d) 0.3, (e) 0.4, and (f) 0.5 eV. The applied electric field is 3×10^5 V/cm.

accordance with the discussions above that carriers move extremely slow near the anode, then gradually speed up.

We further study the effect of the applied voltage V on the inhomogeneity in the internal electric field. The results can be found in Figures S1–S3. As V increases, the carrier density near the anode remains nearly the same. However, the number of carriers across the sample increases. The result is more balanced carriers in the device, leading to a relatively more uniform electric field. This effect is similar to increasing injection barrier. On the other hand, the electric potential becomes parabolic when the applied voltage increases, caused by the higher carrier density across the device.

The trap-free SCL current density is commonly described using the Mott–Gurney equation:[43]

$$J = \frac{9}{8}\varepsilon_0\varepsilon_r\mu\frac{V^2}{L^3} \tag{5}$$

where L is the film thickness. This equation treats carrier mobility as a constant value across the device. Furthermore, the electric field is assumed to be 0 at the anode, because no diffusion is considered. From the results in our simulations, it can be seen that these assumptions are inappropriate.

Figure 4a shows the current density of the simulated device at different electric fields. The mobility is defined as $\mu_{m,SCLC} = \langle\mu\rangle$, which is averaged over the carriers which have crossed the device from the anode to the cathode. $\mu_{m,SCLC}$ is then used to calculate the current density according to the Mott–Gurney equation. Charge mobility depends on the electric field and the carrier density, which we have shown to be highly nonuniform across the device. Furthermore, the enhanced carrier dispersion by high energetic disorders would also greatly affect the charge transport process. All these are not considered in eq 5. It must

dx.doi.org/10.1021/jp5035618 | J. Phys. Chem. C 2014, 118, 9990–9995

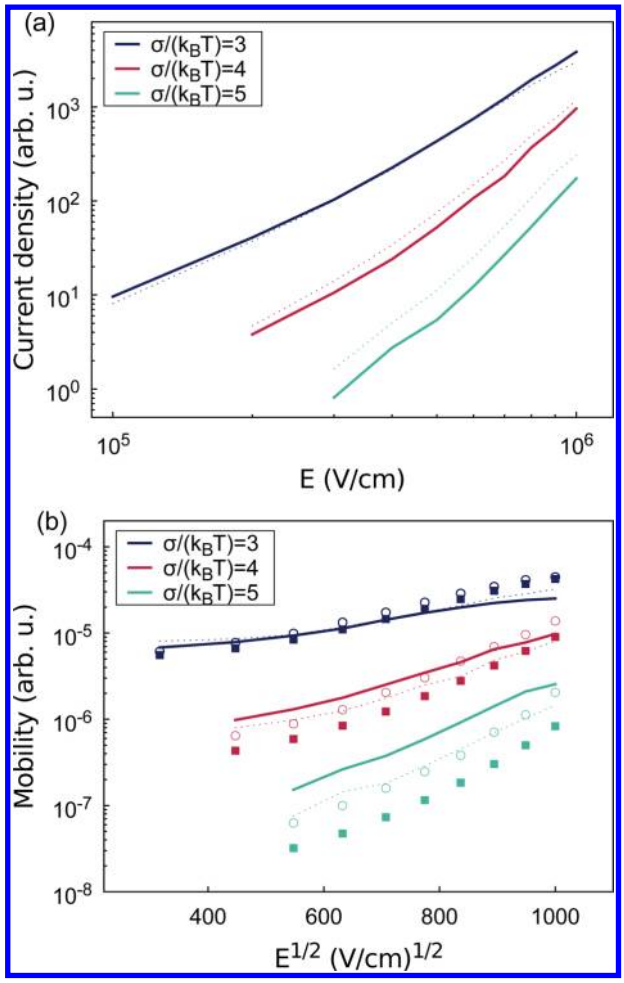

Figure 4. (a) Current density at different applied electric fields. The injection barrier is 0 eV. Dotted lines are calculated according to eq 5 using the mobility averaged over the carriers which have crossed the device. (b) Mobilities from the SCLC simulations: averaged over the carriers which have crossed the device (solid lines) and calculated according to eq 5 from the current density (dotted lines). Mobilities from the TOF simulations: averaged over carriers (filled squares) and calculated using the transit time corresponding to the cross point of the asymptotes to the plateau and trailing edge of the current in the double logarithmic plot (circles). In the TOF simulations, the grid dimension is 188 × 188 × 8000,[15] and the number of carriers is 10.

also be pointed out that the meaning of mobility is different in our simulation. Most carriers just hop back into the same electrode where they are injected from, and only a small portion of them can cross the device. By averaging over the carriers which have reached the cathode from the anode, we risk overestimating the charge mobility. Despite all these differences, it can be seen from Figure 4a that the current density is close to that described by eq 5 when $\sigma/(k_BT) = 3$. As $\sigma/(k_BT)$ increases, J becomes smaller than that predicted by eq 5, which means the apparent mobility (calculated from J according to the Mott−Gurney equation) is lower than $\mu_{m,SCLC}$. However, these results should not be directly compared with those in the work by van Mensfoort and co-workers, who have shown higher current density than the Mott−Gurney equation.[13] The reason is the different meaning of charge mobility in our simulations.

The trap-free SCLC experiment is sometimes preferable when measuring the charge mobility of organic semiconductors, because it has lower requirements on the instruments and the quantity of materials, compared with the TOF measurement. It is intriguing that researchers often find comparable results from the SCLC and TOF measurements,[44,45] although charges transport differently in these cases. To understand the relationship between the mobilities obtained from the SCLC and TOF experiments, we carried out the TOF-type simulations with the same set parameters of the material, where charge injection after $t > 0$ is not allowed and Coulomb interactions are not calculated. The obtained mobility $\mu_{m,TOF}$, which has the same meaning with $\mu_{m,SCLC}$ in the SCLC simulations, is shown in Figure 4b. In the SCLC case, the reversed electric field near the anode slows carrier movement. However, the high carrier density in the device will likely promote charge motion. As a result, $\mu_{m,SCLC}$ and $\mu_{m,TOF}$ are close when $\sigma/(k_BT)$ is not large, as is shown in Figure 4b. However, as $\sigma/(k_BT)$ increases, the enhancement of the carrier density on charge motion is stronger,[33] and the result is that $\mu_{m,SCLC}$ is higher than $\mu_{m,TOF}$.

In experiments, $\mu_{m,SCLC}$ or $\mu_{m,TOF}$ can not be directly obtained. Typically, the mobility is calculated according to eq 5 in the SCLC measurement ($\mu_{exp,SCLC}$), or as $\mu_{exp,TOF} = d/(\tau_{geo}E)$ in the TOF measurement. Here, τ_{geo} is the time corresponding to the cross point of asymptotes to the plateau and trailing edge of the current in the double logarithmic plot. Because the dispersive charge transport, τ_{geo} is smaller than $1/\langle 1/\tau \rangle$[15] This means that $\mu_{exp,TOF}$ is higher than $\mu_{m,TOF}$, which is more obvious at high energetic disorders. As it has been shown above, when $\sigma/(k_BT)$ is large, the apparent mobility $\mu_{exp,SCLC}$ will be lower than $\mu_{m,SCLC}$. As a result, despite the distinctive charge transport processes, $\mu_{exp,TOF}$ and $\mu_{exp,SCLC}$ are surprisingly close (Figure 4b). This explains why the SCLC measurement can lead to similar results compared with the TOF method.[44,45]

In OLEDs, devices are often optimized that the injection barrier is small and the operating voltage is low. At room temperature, most organic semiconductors have $\sigma/(k_BT)$ between 3 and 5.[46−50] This means that, in most OLED devices, the electric field is highly nonuniform. The barrier in the potential surface suppresses the further increase of current density. Methods to eliminate this barrier will increase device performance, which should be taken into account in the future device optimization.

CONCLUSIONS

In summary, using Monte Carlo simulations, we have shown that the electric field is highly inhomogeneous in a hole-only device. A potential barrier is formed near the anode, which suppresses further charge injection. Three factors are found to be effective: the injection barrier (Δ), the energetic disorder (σ), and the applied bias. This potential barrier disappears at low injection degrees, that is, under the condition of a high Δ and a small $\sigma/(k_BT)$. Within the range we studied, the applied voltage is found to reduce the inhomogeneity of the internal electric field by fast drawing carriers from the charge reservoir. Lowering this potential barrier might be a new way to achieve high device performances. It is found that the current density is lower than that predicted by the Mott−Gurney equation for a large $\sigma/(k_BT)$ when our defined mobility $\mu_{m,SCLC}$ is used. Despite the distinctive charge transport processes, the apparent mobilities are found close in both SCLC and TOF simulations, which means that the results from SCLC measurements can be reliable for organic semiconductors.

dx.doi.org/10.1021/jp5035618 | J. Phys. Chem. C 2014, 118, 9990−9995

■ ASSOCIATED CONTENT

Supporting Information

Distribution of charge carriers, electric fields, and potentials at different applied voltages. This material is available free of charge via the Internet at http://pubs.acs.org.

■ AUTHOR INFORMATION

Corresponding Author

*E-mail: duanl@mail.tsinghua.edu.cn. Phone: (+86)10-6277-9988.

Notes

The authors declare no competing financial interest.

■ ACKNOWLEDGMENTS

This research was supported by the National Natural Science Foundation of China (Grant Nos. 51173096, 61177023, and 21161160447). The computation in this research was performed on the "Explorer 100" cluster system of Tsinghua National Laboratory for Information Science and Technology.

■ REFERENCES

(1) Liu, S. H.; Wang, W. C. M.; Briseno, A. L.; Mannsfeld, S. C. E.; Bao, Z. N. Controlled Deposition of Crystalline Organic Semiconductors for Field-Effect-Transistor Applications. *Adv. Mater.* **2009**, *21*, 1217−1232.

(2) Weiss, D. S.; Abkowitz, M. Advances in Organic Photoconductor Technology. *Chem. Rev.* **2010**, *110*, 479−526.

(3) Qiu, Y.; Duan, L. A.; Qiao, J. A.; Sun, Y. D. Strategies to Design Bipolar Small Molecules for Oleds: Donor-Acceptor Structure and Non-Donor-Acceptor Structure. *Adv. Mater.* **2011**, *23*, 1137−1144.

(4) Mishra, A.; Bauerle, P. Small Molecule Organic Semiconductors on the Move: Promises for Future Solar Energy Technology. *Angew. Chem., Int. Ed.* **2012**, *51*, 2020−2067.

(5) Slinker, J. D.; DeFranco, J. A.; Jaquith, M. J.; Silveira, W. R.; Zhong, Y. W.; Moran-Mirabal, J. M.; Craighead, H. G.; Abruna, H. D.; Marohn, J. A.; Malliaras, G. G. Direct Measurement of the Electric-Field Distribution in a Light-Emitting Electrochemical Cell. *Nat. Mater.* **2007**, *6*, 894−899.

(6) Weis, M.; Manaka, T.; Iwamoto, M. Origin of Electric Field Distribution in Organic Field-Effect Transistor: Experiment and Analysis. *J. Appl. Phys.* **2009**, *105*, 024505.

(7) Campbell, I. H.; Joswick, M. D.; Parker, I. D. Direct Measurement of the Internal Electric-Field Distribution in a Multilayer Organic Light-Emitting Diode. *Appl. Phys. Lett.* **1995**, *67*, 3171−3173.

(8) Martin, S. J.; Verschoor, G. L. B.; Webster, M. A.; Walker, A. B. The Internal Electric Field Distribution in Bilayer Organic Light Emitting Diodes. *Org. Electron.* **2002**, *3*, 129−141.

(9) Hoven, C. V.; Peet, J.; Mikhailovsky, A.; Nguyen, T.-Q. Direct Measurement of Electric Field Screening in Light Emitting Diodes with Conjugated Polyelectrolyte Electron Injecting/Transport Layers. *Appl. Phys. Lett.* **2009**, *94*, 033301.

(10) Hiramoto, M.; Koyama, K.; Nakayama, K.; Yokoyama, M. Direct Measurement of Internal Potential Distribution in Organic Electroluminescent Diodes During Operation. *Appl. Phys. Lett.* **2000**, *76*, 1336−1338.

(11) Yin, X. R.; Le, Y. K.; Gao, X. D.; Sun, Z. Y.; Hou, X. Y. Internal Potential Distribution in Organic Light Emitting Diodes Measured by dc Bridge. *Appl. Phys. Lett.* **2010**, *97*, 153305.

(12) Tutis, E.; Berner, D.; Zuppiroli, L. Internal Electric Field and Charge Distribution in Multilayer Organic Light-Emitting Diodes. *J. Appl. Phys.* **2003**, *93*, 4594−4602.

(13) van Mensfoort, S. L. M.; Coehoorn, R. Effect of Gaussian Disorder on the Voltage Dependence of the Current Density in Sandwich-Type Devices Based on Organic Semiconductors. *Phys. Rev. B* **2008**, *78*, 085207.

(14) Li, H. Y.; Duan, L.; Li, C.; Wang, L. D.; Qiu, Y. Transient Space-Charge-Perturbed Currents in Organic Materials: A Monte Carlo Study. *Org. Electron.* **2014**, *15*, 524−530.

(15) Li, H. Y.; Duan, L.; Zhang, D. Q.; Dong, G. F.; Qiao, J.; Wang, L. D.; Qiu, Y. Relationship between Mobilities from Time-of-Flight and Dark-Injection Space-Charge-Limited Current Measurements for Organic Semiconductors: A Monte Carlo Study. *J. Phys. Chem. C* **2014**, *118*, 6052−6058.

(16) Blom, P. W. M.; deJong, M. J. M.; Vleggaar, J. J. M. Electron and Hole Transport in Poly(*p*-phenylene vinylene) Devices. *Appl. Phys. Lett.* **1996**, *68*, 3308−3310.

(17) Blom, P. W. M.; deJong, M. J. M.; vanMunster, M. G. Electric-Field and Temperature Dependence of the Hole Mobility in Poly(*p*-phenylene vinylene). *Phys. Rev. B* **1997**, *55*, R656−R659.

(18) Stossel, M.; Staudigel, J.; Steuber, F.; Blassing, J.; Simmerer, J.; Winnacker, A. Space-Charge-Limited Electron Currents in 8-Hydroxyquinoline Aluminum. *Appl. Phys. Lett.* **2000**, *76*, 115−117.

(19) Mihailetchi, V. D.; van Duren, J. K. J.; Blom, P. W. M.; Hummelen, J. C.; Janssen, R. A. J.; Kroon, J. M.; Rispens, M. T.; Verhees, W. J. H.; Wienk, M. M. Electron Transport in a Methanofullerene. *Adv. Funct. Mater.* **2003**, *13*, 43−46.

(20) Chen, X. W.; Liu, C. Y.; Jen, T. H.; Chen, S. A.; Holdcroft, S. Synthesis and Characterization of a Fullerene Bearing a Triazole Group. *Chem. Mater.* **2007**, *19*, 5194−5199.

(21) Chu, T. Y.; Song, O. K. Hole Mobility of *N*,*N*′-Bis(naphthalen-1-yl)-*N*,*N*′-bis(phenyl) Benzidine Investigated by Using Space-Charge-Limited Currents. *Appl. Phys. Lett.* **2007**, *90*, 203512.

(22) Wang, Z. B.; Helander, M. G.; Greiner, M. T.; Qiu, J.; Lu, Z. H. Carrier Mobility of Organic Semiconductors Based on Current-Voltage Characteristics. *J. Appl. Phys.* **2010**, *107*, 203512.

(23) Silver, M.; Cohen, L. Monte-Carlo Simulation of Anomalous Transit-Time Dispersion of Amorphous Solids. *Phys. Rev. B* **1977**, *15*, 3276−3278.

(24) Schonherr, G.; Bassler, H.; Silver, M. Dispersive Hopping Transport Via Sites Having a Gaussian Distribution of Energies. *Philos. Mag. B* **1981**, *44*, 47−61.

(25) Pautmeier, L.; Richert, R.; Bassler, H. Hopping in a Gaussian Distribution of Energy-States: Transition from Dispersive to Non-Dispersive Transport. *Philos. Mag. Lett.* **1989**, *59*, 325−331.

(26) Pautmeier, L.; Richert, R.; Bassler, H. Poole-Frenkel Behavior of Charge Transport in Organic-Solids with Off-Diagonal Disorder Studied by Monte-Carlo Simulation. *Synth. Met.* **1990**, *37*, 271−281.

(27) Pautmeier, L.; Richert, R.; Bassler, H. Anomalous Time-Independent Diffusion of Charge-Carriers in a Random Potential under a Bias Field. *Philos. Mag. B* **1991**, *63*, 587−601.

(28) Meng, L. Y.; Wang, D.; Li, Q. K.; Yi, Y. P.; Bredas, J. L.; Shuai, Z. G. An Improved Dynamic Monte Carlo Model Coupled with Poisson Equation to Simulate the Performance of Organic Photovoltaic Devices. *J. Chem. Phys.* **2011**, *134*, 124102.

(29) Novikov, S. V.; Tyutnev, A. P.; Schein, L. B. Time of Flight Transients in the Dipolar Glass Model. *Chem. Phys.* **2012**, *403*, 68−73.

(30) Hoffmann, S. T.; Athanasopoulos, S.; Beljonne, D.; Bassler, H.; Kohler, A. How Do Triplets and Charges Move in Disordered Organic Semiconductors? A Monte Carlo Study Comprising the Equilibrium and Nonequilibrium Regime. *J. Phys. Chem. C* **2012**, *116*, 16371−16383.

(31) Gagorik, A. G.; Mohin, J. W.; Kowalewski, T.; Hutchison, G. R. Monte Carlo Simulations of Charge Transport in 2d Organic Photovoltaics. *J. Phys. Chem. Lett.* **2013**, *4*, 36−42.

(32) Mendels, D.; Tessler, N. Drift and Diffusion in Disordered Organic Semiconductors: The Role of Charge Density and Charge Energy Transport. *J. Phys. Chem. C* **2013**, *117*, 3287−3293.

(33) Pasveer, W. F.; Cottaar, J.; Tanase, C.; Coehoorn, R.; Bobbert, P. A.; Blom, P. W. M.; de Leeuw, D. M.; Michels, M. A. J. Unified Description of Charge-Carrier Mobilities in Disordered Semiconducting Polymers. *Phys. Rev. Lett.* **2005**, *94*, 206601.

(34) Bassler, H. Charge Transport in Disordered Organic Photoconductors—A Monte-Carlo Simulation Study. *Phys. Stat. Solidi B* **1993**, *175*, 15−56.

(35) Coropceanu, V.; Cornil, J.; da Silva, D. A.; Olivier, Y.; Silbey, R.; Bredas, J. L. Charge Transport in Organic Semiconductors. *Chem. Rev.* **2007**, *107*, 926−952.
(36) Tessler, N.; Preezant, Y.; Rappaport, N.; Roichman, Y. Charge Transport in Disordered Organic Materials and Its Relevance to Thin-Film Devices: A Tutorial Review. *Adv. Mater.* **2009**, *21*, 2741−2761.
(37) Houili, H.; Tutis, E.; Batistic, I.; Zuppiroli, L. Investigation of the Charge Transport through Disordered Organic Molecular Heterojunctions. *J. Appl. Phys.* **2006**, *100*, 033702.
(38) Gonzalez-Vazquez, J. P.; Anta, J. A.; Bisquert, J. Random Walk Numerical Simulation for Hopping Transport at Finite Carrier Concentrations: Diffusion Coefficient and Transport Energy Concept. *Phys. Chem. Chem. Phys.* **2009**, *11*, 10359−10367.
(39) Kimber, R. G. E.; Wright, E. N.; O'Kane, S. E. J.; Walker, A. B.; Blakesley, J. C. Mesoscopic Kinetic Monte Carlo Modeling of Organic Photovoltaic Device Characteristics. *Phys. Rev. B* **2012**, *86*, 235206.
(40) Miller, A.; Abrahams, E. Impurity Conduction at Low Concerntrations. *Phys. Rev.* **1960**, *120*, 745−755.
(41) Zhou, J.; Zhou, Y. C.; Zhao, J. M.; Wu, C. Q.; Ding, X. M.; Hou, X. Y. Carrier Density Dependence of Mobility in Organic Solids: A Monte Carlo Simulation. *Phys. Rev. B* **2007**, *75*, 153201.
(42) van der Holst, J. J. M.; van Oost, F. W. A.; Coehoorn, R.; Bobbert, P. A. Monte Carlo Study of Charge Transport in Organic Sandwich-Type Single-Carrier Devices: Effects of Coulomb Interactions. *Phys. Rev. B* **2011**, *83*, 085206.
(43) Lampert, M. A.; Mark, P. *Current Injection in Solids*; Academic Press: New York, 1970.
(44) Tse, S. C.; Tsung, K. K.; So, S. K. Single-Layer Organic Light-Emitting Diodes Using Naphthyl Diamine. *Appl. Phys. Lett.* **2007**, *90*, 213502.
(45) Schwartz, G.; Ke, T. H.; Wu, C. C.; Walzer, K.; Leoc, K. Balanced Ambipolar Charge Carrier Mobility in Mixed Layers for Application in Hybrid White Organic Light-Emitting Diodes. *Appl. Phys. Lett.* **2008**, *93*, 073304.
(46) Mozer, A. J.; Sariciftci, N. S.; Pivrikas, A.; Österbacka, R.; Juška, G.; Brassat, L.; Bässler, H. Charge Carrier Mobility in Regioregular Poly(3-hexylthiophene) Probed by Transient Conductivity Techniques: A Comparative Study. *Phys. Rev. B* **2005**, *71*, 035214.
(47) So, S. K.; Tse, S. C.; Tong, K. L. Charge Transport and Injection to Phenylamine-Based Hole Transporters for Oleds Applications. *J. Displ. Technol.* **2007**, *3*, 225−232.
(48) Chen, L.; Dong, G. F.; Duan, L.; Qiao, J.; Zhang, D. Q.; Wang, L. D.; Qiu, Y. Positional Disorder-Induced Mobility Enhancement in Rapidly Cooled Organic Semiconductor Melts. *J. Phys. Chem. C* **2010**, *114*, 9056−9061.
(49) Chan, K. K. H.; Tsang, S. W.; Lee, H. K. H.; So, F.; So, S. K. Charge Injection and Transport Studies of Poly(2,7-carbazole) Copolymer PCDTBT and Their Relationship to Solar Cell Performance. *Org. Electron.* **2012**, *13*, 850−855.
(50) Chan, C. Y. H.; Tsung, K. K.; Choi, W. H.; So, S. K. Achieving Time-of-Flight Mobilities for Amorphous Organic Semiconductors in a Thin Film Transistor Configuration. *Org. Electron.* **2013**, *14*, 1351−1358.